LBNL 2019(2022) inter-laboratory comparison for laboratories submitting specular data to the IGDB

Jacob C. Jonsson
Lawrence Berkeley National Laboratory

Windows and Envelope Materials Group
Building Technology Department
Building Technology and Urban Systems Division
Energy Technologies Area

June 14, 2022

Disclaimer

Abstract

This report covers the process and result of the LBNL run inter-laboratory comparison (ILC) between measurement laboratories characterizing the solar optical properties of glass and glazing products.

Numerical results are from the most recent (2019-2022) ILC, but it includes findings from older studies as well. It is considered an important part of this process to educate and improve the results from laboratories that suffer from systematic errors in their results. Collecting both common and rare problems in this document is meant to serve as help for troubled spectroscopists.

One new study that was enabled in this round was the spread of measurement over a two-year time span. Concerns that low-e coatings would age significantly over this time was taken seriously and graphs showing results versus measurement date are included. Excluding a few samples that were visibly damaged, it seems like the aging was insignificant with respect to the aging of the coatings.

1 Introduction

Laboratories that submit data to the International Glazing Database (IGDB) have to participate in an inter-laboratory comparison (ILC) every four years. This is a procedure that allow both contributors and database maintainers to confirm that the measurement capabilities of the laboratories are of high quality.

The IGDB contains optical information in the wavelength region between 300-2500 nm where transmittance as well as reflectance for both the front and the back surface is recorded. In addition to that emissivity, obtained through measurement of reflectance between 5 and 25 μm, is recorded for both the front and back surface.

The goal for submitters is to pass within the tolerances dictated by NFRC document 302 which states that transmittances should be within 1% and reflectance/emissivity within 2%. As an organizing entity LBNL aims to educate and help submitters troubleshoot any issues that give rise to systematic errors.

The ILC is a living ILC and does not necessarily contain the first result submitted by a lab. As errors are found submitters are encouraged to correct procedures or update equipment so that they are allowed to submit data to the IGDB. The risk of this practice is that if any of the recommended solutions introduces new systematic errors this will start to influence the average. Therefore this report tries to highlight the recommendations made so that they can be challenged.

Normally an ILC does not take 3 years to carry out. Samples were sent out in December 2019, but due to the outbreak of Covid-19 the activity was paused in the spring of 2020. The decision to restart it again came in fall of 2021 as it was expected that participants that needed to participate had controls in place to do so in a safe manner in contrast to waiting until the pandemic was over.

2 Samples

The ILC was a parallel ILC, i.e. all participants get their own set of samples. This has proven valuable in the past for the participants since they can go back and remeasure their samples after moving or modifying their measurement equipment.

2.1 Specular sample selection

A total of three samples were selected to show to show high and low transmittance, variation between visible and NIR, and different level of thermal IR reflectance. The clear glass is stable and should have minimum sample variation and be stable over time. The low-e coatings were of different design to give two data points on the emissivity. The uncoated side is designated as front. To summarize:

1. 3 mm clear monolithic glass

2. 3 mm coated with lower solar gain

3. 3 mm coated with higher solar gain

In the 2011 and 2015 ILCs approximately 45 boxes were sent out initially and the total number grew to over 60 over the 4 years. For the 2019 we prepared 80 boxes and send out 41 boxes initially, and an additional 7 were sent out when the activity was resumed at the end of 2021. The remaining boxes are kept at LBNL for future inclusion of participants.

2.2 Sample variation

Transmittance measurements of each sample was carried out at 550 nm to give an indication of the sample variation, this was done at LBNL before samples were shipped out. The transmittance was measured for 20 seconds with the signal sampled every second, typical variation in reading over 20 seconds was ± 0.0002. The difference between samples and the average was calculated by subtracting the mean from each measured value. The extreme values as well as two times the standard deviation is shown in figure 1.

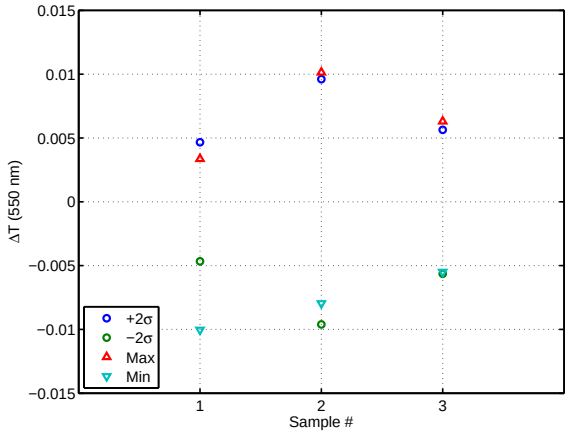

Figure 1: Statistics of the absolute variation of transmittance measured at 550 nm for the different samples.

The variation of the glass samples were small. All in all, more than 90% of the samples were within 0.005 absolute difference from the mean value. The outliers among the low-e coatings is believed to be due to defects from shipping and handling the samples. The conclusion from looking at this data is that it is of little benefit to force the manufacturers to measure more than one sample.

After the variation had been measured at LBNL, the samples where packaged, shipped, and upon reception cleaned by the recipient before they measured it with their instrument.

As measurements were submitted under a long time span we took the opportunity to see if there were any signs of degradation in the low-e coatings. This was not a planned

experiment and therefor lacks rigorous control to remove other factors relating to degradation, e.g. different storage conditions and handling.

3 Solar optical range, 300–2500 nm

3.1 Instruments and detectors used

A majority of the ILC participants used Perkin-Elmer Lambda 900/950/1050 instruments fitted with a 150 mm integrating sphere. The low number of other instrument types limits the ability to draw conclusions from the results. A breakdown is shown in figure 2a). Instruments with zero occurrences were included in the graph for one of two reasons, either it was present in a past ILC or its user did not submit data before this report was finalized. This is not an attempt to list all possible instruments available.

The typical detector combination is a photo multiplier tube (PMT) for the visible range and a lead sulfide (PbS) detector for the NIR. The Lambda 1050 instruments feature an indium gallium arsenide (InGaAs) detector instead. All participants had an integrating sphere, the diameter distribution is shown in figure 2b).

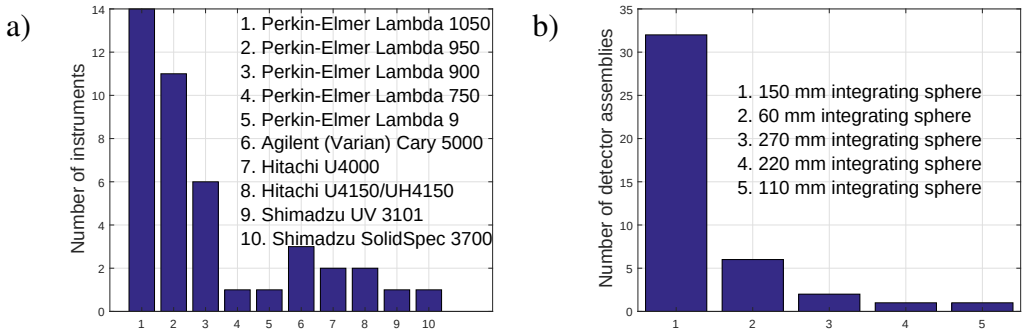

Figure 2: a) Distribution of instruments among the participants. b) Distribution of detector systems used.

With such a dominance of a few detector systems and instruments it is impossible to confidently say that the other instruments and detectors are performing better or worse. No error was tied to a single brand or detector type.

3.2 Example of results

The full results for UV, visible, and near infrared results are show in appendix B.

An example of the wavelength resolved data is shown in figure 3. Each participant get these graphs to show their individual results compared to an average over the set. Looking at the specular results give information that can be used to identify systematic errors as discussed in section 3.4. The dashed lines are an average of the spectra participants without systematic errors. As the number of participants grow over time it has been noted by

early submitters that the average they see in their individual graph does not exactly match the average shown in the final report. While this is not ideal, it is preferred to give rapid feedback to early submitter rather than waiting for the final deadline.

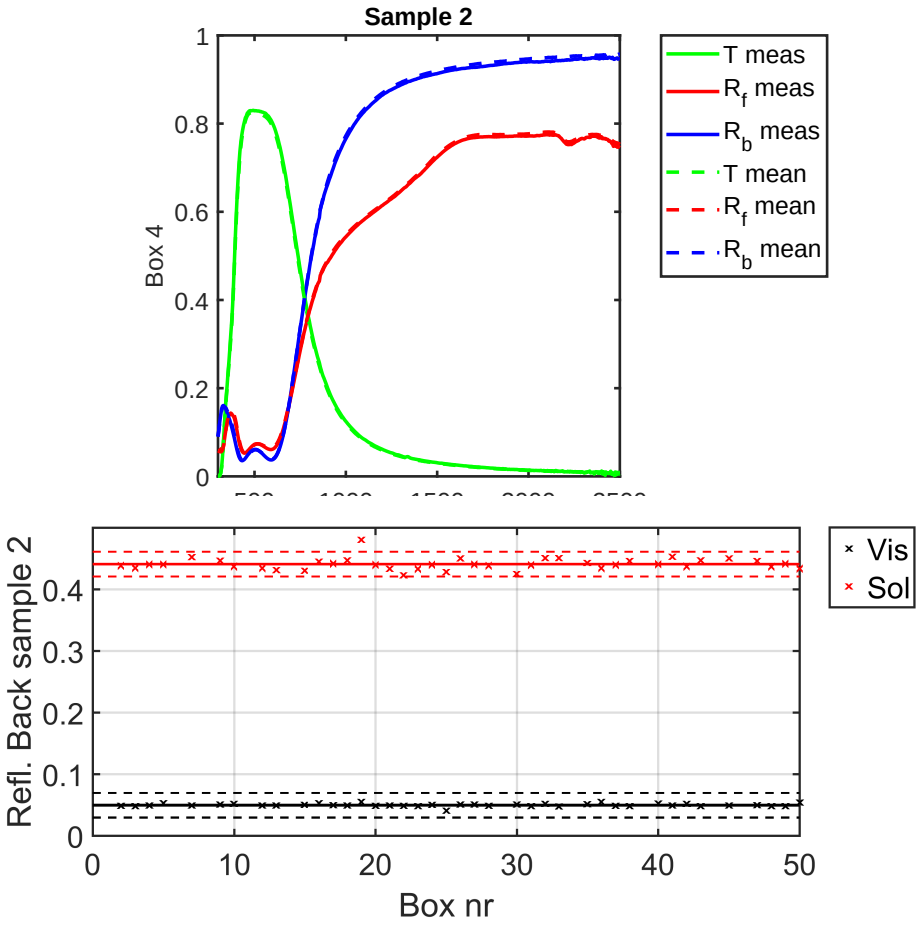

Figure 3: a) Example of spectral data for a single submitter (solid lines) compared to the average spectral data of non-outlier participants (dashed lines). b) Integrated visible and solar value for all participants. The dashed lines mark the NFRC 302 allowed tolerance.

3.3 Lessons from past ILCs

This section collects past and present conclusions that can be shown using data sets of this type.

3.3.1 Effects of large wavelength steps when measuring applied films

LBNL used to allow steps of 50 nm or shorter for data at wavelengths longer than 1000 nm. The consequences of using the longest step length is shown in figure 4b); with very narrow interference fringes it is more or less random what value is reported in the range from high to low.

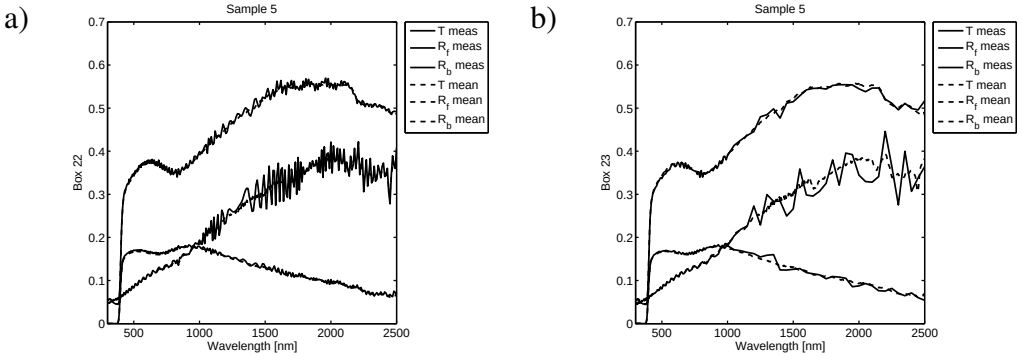

Figure 4: Data for the 2011 applied film sample. a) Data presented with 5 nm steps. b) Data presented with 50 nm steps.

There are two ways to avoid this, the practical way is to measure at shorter steps, as shown in figure 4a), which makes it less probable that streaks of high or low values will skew the integrated values.

The second way is to adjust the bandwidth of light used to illuminate the sample. The grating of a spectrophotometer in practice produces a distribution of wavelengths and the bandwidth of this is controlled by a slit in the optical system. This will create an average over multiple wavelengths which creates a smoother curve. While not an accurate representation of the interference fringes it will produce accurate results for integrated values.

3.3.2 Diffuse versus specular reference

The results form this section were obtained in the 2015 ILC.

Integrating sphere theory suggests that using a diffuse reference sample of the same material as the sphere wall will give you an absolute reflectance measurement for specular samples. This requires that the detector response is identical for light incident on the specular port and the reflectance sample position. Since commercial integrating spheres are not ideal spheres it is not obvious that it would give the same result as when using a specular reference mirror. Data from this ILC can be used to compare results using diffuse standards, first surface mirrors, and second surface mirrors.

The specular mirrors have been divided between first, or front, surface mirrors and second surface mirrors. For the first surface mirrors the mirror film is exposed to air and will be in direct contact with the instrument. Even though some of these mirrors are

protected with a surface coating they are sensitive to scratching which can occur when mounting against the sphere wall. The second surface mirrors have the mirror film sealed on the back of a transparent substrate. This protection results in a slightly lower reflectance but makes the mirror less sensible to degradation.

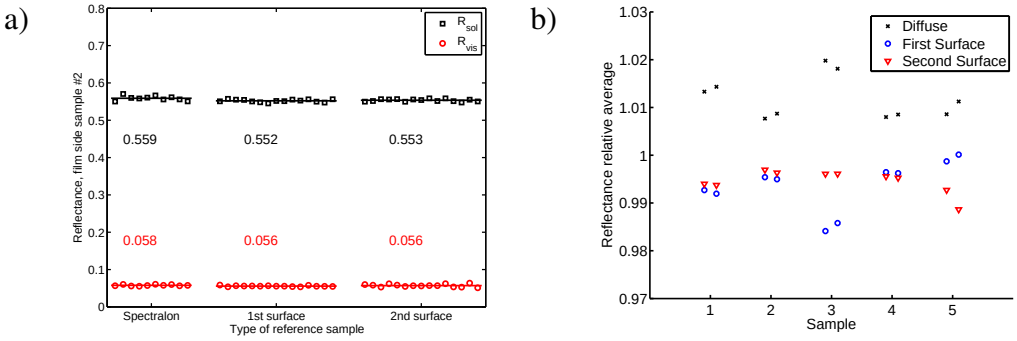

Figure 5: Integrated reflectance grouped for kind of reference sample. The average value for each group is written next to the curve. The diffuse Spectralon group has a slightly higher average than the other two. a) Film-side reflectance of sample #2 showing the individual measurements for each participant. b) Showing the reflectance relative the average for that sample for all measured reflectances. The two values for each sample is front and back reflectance. (Graphs from the 2011 ILC).

The reflectance measured is graphed versus the type of reference used in figure 5. The metal coating of sample #2 is shown in figure 5a) and the solar reflectance is slightly higher, about .005 or 1% relative, on average but the visible reflectance is seemingly independent of reference sample. In figure 5b) the average of each group is graphed divided by the average for all groups. It shows that for all 10 measured reflectance values, counting front and back of the five samples, the data submitted using a Spectralon reference is consistently higher than average and the specular mirrors are lower.

One way to get a value that is too high is if the reference sample has a lower reflectance than it is supposed to. In the case of a specular reference mirror that happens if the surface has a lower reflectance than its certificate. In the case of a diffuse reference sample it happens if the Spectralon reference has a lower reflectance than the specular port. By lower reflectance in this case it is not only necessary to consider the actual reflectance of the material but also the response from the detector in the integrating sphere. So the sphere geometry coupled with the scattering distribution of the material, both the reference and the specular port, could play a role in any deviation from the true value.

It has been shown that Spectralon reflectance decreases with time even if the material is kept in the dark[1]. One possible hypothesis is that the Spectralon reference deteriorates faster than the specular port due to handling and that this gives rise to a systematically too high measured reflectance. Another possibility is that the detector response is different for light scattered from the specular port and the sample port.

Without a definite way to insure that the Spectralon absorption bands does not start to influence the result, it is highly recommended that a second surface mirror is used.

3.4 Example of corrected results

This section highlights some of the systematic errors that have occurred and suggested methods how to fix them. Some of these show up repeatedly but can be hard to replicate on different instruments.

3.4.1 Misaligned grating

The correlation between the mechanical position of the monochromator diffraction grating and the recorded wavelength of each measurement point has to be calibrated. Typically this is done using a sample with very sharp absorption peaks, e.g. a Holmium Perchlorate solution, or an emission light source, e.g. a Deuterium lamp. The instrument software correlates its reading of the grating position with the known position of the peaks.

The grating usually does not lose its position but, e.g. if it is moved and gets bumped or if dust is building up in the mechanical system, it is a good idea to run a calibration. Some software suggests that you do this with a fixed frequency which is not a bad idea.

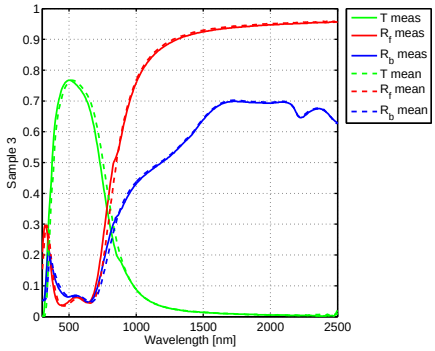

Figure 6: The slopes of the measured data are offset with respect to each other.

There are some ways to spot if the grating is out of alignment without running the calibration. One is to look at sample properties with a significant derivative in grating change region. An example of this is shown in figure 6. This does not tell you which grating is out of alignment, but it signals that something is wrong. More about discontinuities in section 3.4.2. On the other hand, if both are the same amount out of sync there might be no discontinuity so this is not a sufficient test to say that the instrument is aligned, only a way to spot that it is not.

Some Perkin-Elmer instruments have a 0 nm wavelength setting where the grating is parallel to the beam to let it pass through as white light (also called alignment mode). If the calibration is sufficiently off this can result in the grating fully or partially blocking the beam resulting in no visible beam.

3.4.2 Discontinuity at grating change

These spectrophotometers are built to cover two wavelength ranges and mechanical alignment of detectors, gratings, and light sources is an engineering problem that is part of the challenge of building these instruments.

Example of a couple of different instrument results are shown in figure 7a) A step of .02 indicates that you have no room for sample variation if you want to stay within .02 tolerance. Smaller steps are unsightly and could create problems for calculation of optical constants or when deconstructing an applied film or a laminate.

The step shown in figure 7b) was reduced by using a fixed slit width in NIR rather than the default servo setting. It also mattered what the ratio of slit width between the two gratings, best results were obtained when the ratio matched the ratio between the number of grooves per mm for the gratings. This keeps the light spot the same size.

The gratings also have a strong polarizing effect, if the instrument is not fitted with a depolarizer and the sample is polarized there is a possibility that there will be a discontinuity here as well.

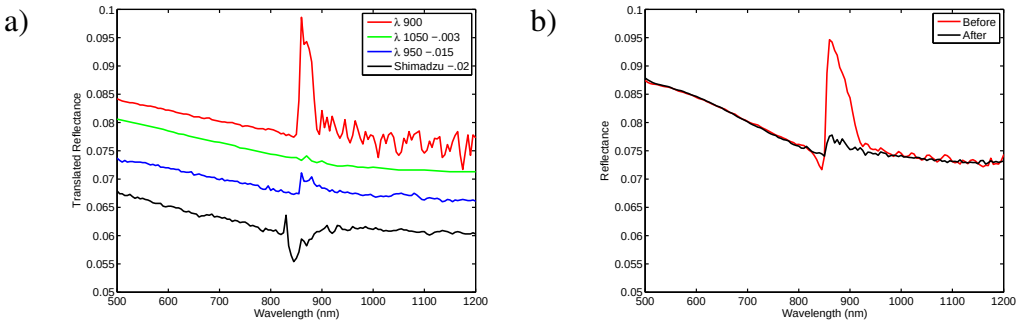

Figure 7: a) Example of different glass reflectance measurement of sample #1, values have been shifted laterally to clearer show the discontinuities. b) Example from a measurement in the ILC conducted in 2007.

3.4.3 Absorption artifacts in NIR

Sample #2 has an exposed metal coating that is highly reflective in NIR. The flat shape of the reflectance for the coated side makes it easy to spot any absorption artifacts in that range. An example of the effect is shown in figure 8 from a metal coated sample used in the ILC 2007, sample #2 in this ILC has similar properties but very few submissions showed this effect so far this year which is why it is exemplified using data from 2007.

It is hard to repeat this effect but a theory for how this happens is suggested. The submissions in figure 8 all used a diffuse reference and a Spectralon integrating sphere. In theory this should give the reflectance value assuming the detector response is the same for light incident on the reference sample and the specular port[1]. These two sphere locations are both baffled and not directly in the detector field of view and in those cases the most plausible explanation would be that the reference and the port have degraded differently.

[1]It is common, but not necessary that an integrating sphere has a specular port, if none is present it is the sphere wall at the spot where the specular reflection first interacts with the sphere that has to have the same detector response as the reference sample

Some submitters tried to clean their reference samples but without any improvement. The only way they could get accurate results was to use a specular reference mirror.

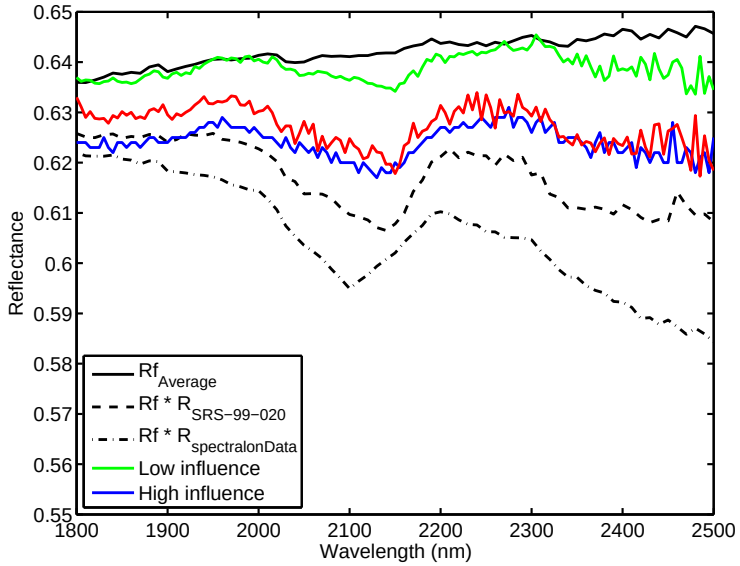

Figure 8: Average reflectance of a metal coated glass substrate and that value multiplied with the reflectance of Spectralon contrasted against submissions with absorption artifacts.

3.4.4 Sample holder increasing reflected value

Different spectrophotometers use different methods to mount samples in the optical path. One design, which has benefits with regards to the acceptable sample dimensions, is based on clamping the sample to the integrating sphere wall. Despite the benefits, there is chance that the clamp gets into the beam path and in combination with a transparent sample it might give an error in measured reflectance.

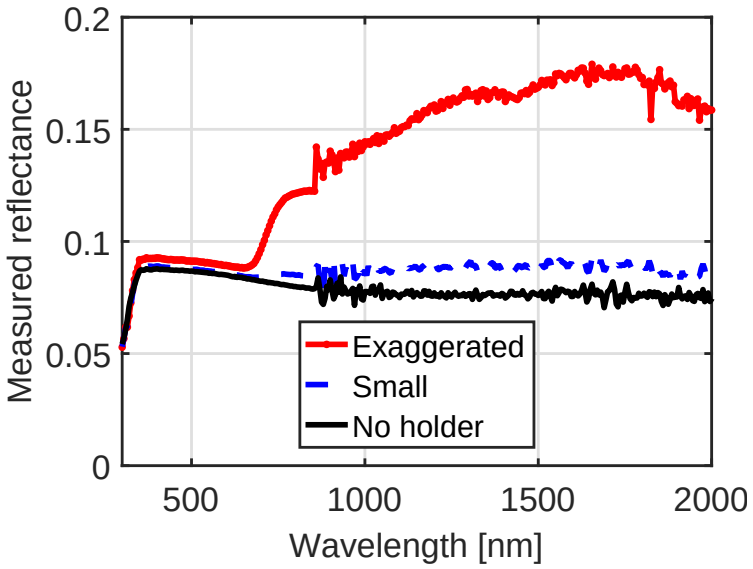

Figure 9: Reflectance of glass measured with clamping sample holder contributing to the recorded value. The *Rxaggerated* curve was captured with the sample holder deliberatly out of position, the *Small* curve was done with more typical misalignment. The sample was not *No holder* curve

Three measurements were made of the same sample to demonstrate the effect, the results are shown in figure 9. Not using the clamping holder at all gives a baseline measurement to compare with two incorrect measurements. The exaggerated measurement has not been seen in the ILCs, but the small effect has been seen every now and then.

There are multiple solutions that can resolve this issue. Careful use of the clamp to make sure it is sufficiently centered on the sample and that there is no interaction with the beam. Modifying the clamp or building a different mounting system might be worth it if the flexibility of the existing clamp is not required.

However, if the beam does occasionally interact with the sample holder it could be an indication that the beam alignment is not well centered, and it is recommended that an alignment check is carried out.

It is possible to do a separate zero measurement in an attempt to subtract the impact of the sample holder. While good practice, and commonly part of instrument measurement procedures, this is not recommended as a solution to this issue as it is unlikely that the clamp will be in exactly the same position depending on the presence of a sample or not.

4 Thermal infrared range, 5–25μm

4.1 Instruments used

The IR instrument market is more diverse than the solar optical instrument market and that is seen in the range of instruments used presented in figure 10. Instruments with zero occurrences were included in the graph for one of two reasons, either it was present in a past ILC or its user did not submit data before this report was finalized. This is not an attempt to list all possible instruments available.

The THERMES project[2, 3, 4] did thorough comparisons between dispersive and FTIR instruments and those have not been repeated here since there were too few dispersive instruments in this data set.

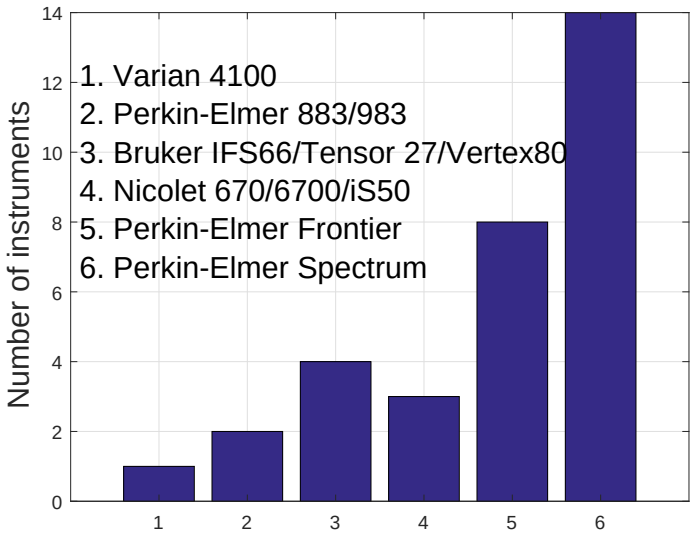

Figure 10: Distribution of instruments used to measure reflectance between $5\mu m$ and $25\mu m$ for calculation of emissivity.

There was a call for submission using emissometer type instruments but only two boxes were measured using those. The results from those two boxes were good but without a larger set of participants it is optimistic to draw any conclusions.

4.2 Emissivity calculations

The IGDB contains information about the emissivity in the infrared range. To obtain this value reflectance is measured and since the samples are opaque in the infrared wavelength region so the absorption is equal to one minus the reflectance. The spectral absorption is weighted using a 300 K black body curve according to NFRC 301[5]. This temperature is the default in the LBNL Optics/Window 5 programs. The IGDB allows submissions where the submitter has calculated the emissivity instead of submitting the measured data.

The calculation of emissivity is not always carried out in this way. The European standard EN673[6] uses a temperature of $283K$ instead of $300K$. A room-temperature blackbody emits about 17% of the total energy at longer wavelengths than $25\mu m$, if the region is extended to $40\mu m$ a different value can be obtained for some materials. The difference in calculated emissivity for low-e coatings is very small though as there is next to no variation in reflectance beyond $25\mu m$. The numerical differences are shown in figure 11 for a single data file from this ILC. The reason to not measure beyond $25\mu m$ is purely practical in that for a long time it was impossible to purchase a new IR spectrophotometer that could measure longer wavelengths.

The conclusions to draw is that even though the differences are not large it could lead to rounding differently depending on how the emissivity was calculated.

All the emissivity values are shown in appendix C and in those graphs it is also possible to see which values were submitted spectra and which were submitted as calculated values.

In addition to the choice of black body temperature there is also a transformation from the direct emissivity (which is measured) to the hemispherical emissivity which is the reported property. This is carried out in accordance to NFRC 301[5].

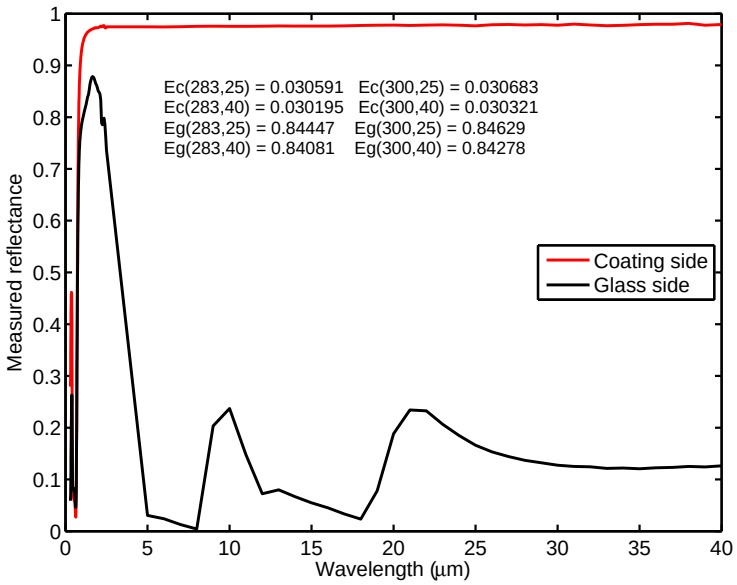

Figure 11: Spectral reflectance measured and hemispherical emissivity calculated for two temperatures, 283 K and 300 K, and using two different upper boundaries for the calculation. The calculation was carried out for both the glass side (E_g-values) and the coated side (E_c-values) of the sample.

4.3 Measurements

Out of the three samples, there were four uncoated surfaces. By measuring glass emissivity 4 times the laboratories got good information about how the repeatability of the instrument was. An example of such a result is shown in figure 12.

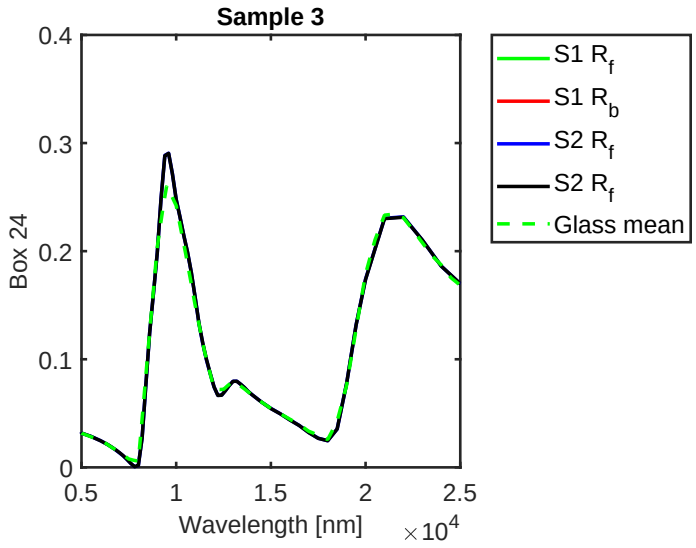

Figure 12: Example of submitter number 24's reflectance measurement of the 5 uncoated glass surfaces all show together in one graph to demonstrate the instrument variation.

In addition to the glass reflectance the low-e coating was graphed individually. Examples of that measurement is shown in figure 13.

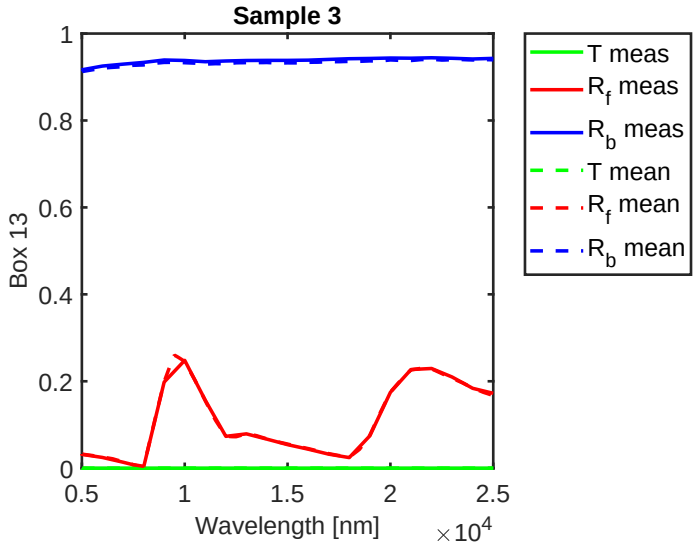

Figure 13: Example of submitted IR reflectance of the low-e coating. Properites marked $meas$ are the submitter's measured values of the surfaces and it is compared to the average of all non-outlier submitters measured values $mean$. The index $_f$ and $_b$ indicates film side.

4.4 Calculation of hemispherical emissivity

A two step process is used to calculate the hemispherical emissivity from the near normal IR reflectance measurement measured. For the IGDB we calculate this value according to NFRC 301. To obtain corrected emissivity values according to EN 12898 the process from measurement to final value is different, but not covered here.

4.4.1 Calculation of normal emissivity

The normal emissivity is calculated by integrating the measured reflectance, $R(\lambda)$, weighted with the black-body emissivity spectrum of a 300 K body, $E_b(\lambda)$, according to

$$\varepsilon_n = \frac{\int_{5\mu m}^{25\mu m}(1 - R(\lambda))E_b(\lambda)\,d\lambda}{\int_{5\mu m}^{25\mu m} E_b(\lambda)\,d\lambda}, \tag{1}$$

where $E_b(\lambda)$ is calculated according to

$$E_b(\lambda) = \frac{C_1}{\lambda^5\left(\varepsilon^{C_2/\lambda T}\right)}, \tag{2}$$

where the emitted black-body radiation, $E_b(\lambda)$, is given by

C_1 Planck's first constant ($3.743 \times 10^8 W\mu m^4/m^2$)

C_2 Planck's second constant ($1.4387 \times 10^4 mumK$)

T temperature (K)

λ wavelength (μm).

4.4.2 Conversion from normal to hemispherical emissivity

The hemispherical emissivity, rather than the normal emissivity, is the property used in thermal calculations. Rather than to measure the hemispherical value it is calculated from the normal emissivity using empirical expressions[7].

For uncoated substrates the expression is:

$$\varepsilon_h = 0.1569\varepsilon_n + 3.7669\varepsilon_n^2 - 5.4398\varepsilon_n^3 + 2.47333\varepsilon_n^4 \tag{3}$$

where ε_n is the normal emissivity calculated using equation 1.

For coated substrates the expression is:

$$\varepsilon_h = 1.3217\varepsilon_n - 1.8766\varepsilon_n^2 + 4.6586\varepsilon_n^3 - 5.8349\varepsilon_n^4 + 2.7406\varepsilon^5. \tag{4}$$

4.4.3 Calculated emissivities for samples 1–3

All calculated hemispherical emissivity values are presented in appendix C. The average value for the low-e coated surface of sample 2 and sample 3 were 0.039 and 0.082, respectively. The average glass emissivity was 0.844.

4.4.4 Emissivity as a function of measurement date

A major concern during this effort was the aging of the coatings as the effort dragged out due to Covid. However, only a few participants needed a new box sent out due to the aging of the samples. Part of that was poor packaging on my part, some samples had plastic bubble wrap in contact with the sample which left round pock-marks on the surface.

Luckily a fair number of participants managed to measure and submit before the activity was postponed. Other participants were submitting throughout the pandemic and then there was a bump again as a 2022 deadline was set. With this spread of results over time it is helpful to graph the results over time to see if there was an trend in the result.

The mathematically approach was to fit a first order polynomial to the data and look at the slope of that fit. Data and polynomial fits are shown in figure 14. That the slope of the coated surface (a) and the uncoated side (c) for sample 2 is the same makes it unlikely that there is a significant aging skewing the result for sample 2.

The coated side for sample 3 was slightly trickier as seen in figure 14b). One outlier was identified (over 0.13) and the participant confirmed that the surface was damaged and they had failed to find an undamaged part of the surface to do the IR measurement on. Excluding that data point gives a negative slope for the emissivity versus time measurements.

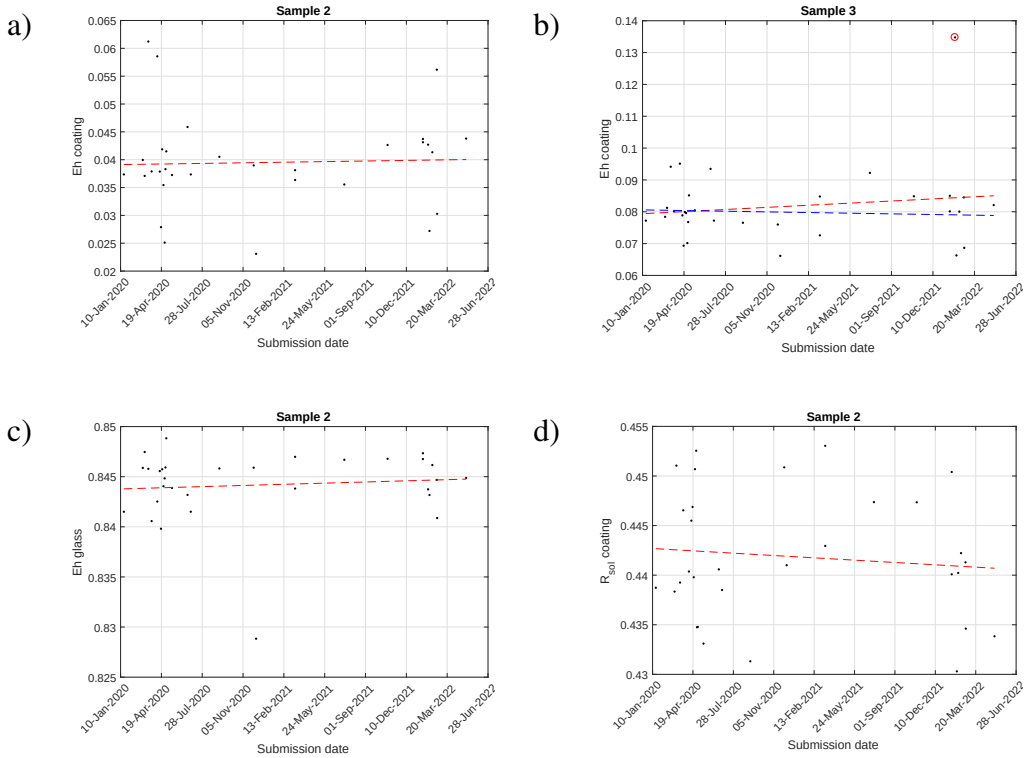

Figure 14: a) and b) Eh versus measurement date for the coated side sample 2 and 3, respectively. c) Eh of the uncoated surface for comparison. d) Rsol of the coated surface for sample 3.

A less thorough investigation was carried out on the solar transmittance and reflectance values, only the sample 2 solar reflectance is shown infigure 14d). There was a negative trend demonstrated but it was also small compared to the tolerance.

This brief investigation does not prove that there was no deterioration of the samples due to aging, but it was interpreted as that if there was aging it did not invalidate the ILC activity. A few participants were unable to measure on an undamaged part of the sample and those participants were sent new boxes.

While this was educational and did not seem to ruin the activity, it is not a recommendation for increasing the traditional measurement deadline for ILCs.

5 Conclusions

This report indicates that the state of the participants measurements is in general very healthy, almost all measurements are within the tolerances set by NFRC.

It is the intent of LBNL to work with ISO and ASTM standards groups to improve on the language in standards to make it easier for new submitters to find information in

the right place on how to carry out good measurements, and if possible prove that the tolerances could be decreased.

6 Acknowledgement

This work was financed by NFRC and supported in part by the Assistant Secretary for Energy Efficiency and Renewable Energy, Building Technologies Program of the U.S. Department of Energy under Contract No. DE-AC02-05CH11231.

Samples were provided by a manufacturer that preferred to not be listed.

All participants contributed significant time in measuring all sample properties.

References

[1] W. Möller, K. Nikolaus, and A. Höpe, "Degradation of the diffuse reflectance of spectralon under low-level irradiation," *Metrologia* **40**, pp. 212–215, 2003.

[2] "THERMES, thermal emissivity of energy-saving coatings on glass - preservation of the measuremnt infrastructure of the glazing industry," tech. rep., EU Growth Programme Contract G6RD-CT-2001-00658, 2001.

[3] K. Gelin, A. Roos, P. van Nijnatten, and F. Geotti-Bianchini, "Thermal emittance of coated glazing - simulation versus measurement," *Optical Materials* **27**, pp. 705–712, 2005.

[4] P. van Nijnatten, M. Hutchins, A. Roos, F. Geotti-Bianchini, P. Polato, C. Anderson, F. Olive, M. Köhl, R. Spragg, and P. Turner, "Thermal emissivity of energy-saving coatings on glass: The THERMES project," in *4th International Conference on Coatings on Glass*, 2002. Braunschweig, Germany.

[5] National Fenestration Rating Council, "NFRC301-2020[E0A0]: Standard test method for emittance of glazing products," 2020.

[6] European Committee for Standardization, "EN673: Glass in building - determination of thermal transmittance (u value) - calculation method," 1997.

[7] M. Rubin, D. Arasteh, and J. Hartmann, "A correlation between normal and hemispherical emissivity of low-emissivity coatings on glass," *Int. Comm. Heat Mass Transfer* **14**, pp. 561–565, 1987.

Appendix

A List of Participants

Table 1: Autogenerated table from what participant wrote in the *boxnninfo.txt* file. Not listed in box number order.

Institute	**Contact**
AGC Glass Co. Japan/Asia Pacific	Sigetosi Hirasima
AGC glass Europe	Ingrid Marenne
arcon Flachglas-Veredlung GmbH & Co.KG	Christian Mueller
BCRC (Belgian Ceramic Research Centre)	Dominique Libert
Cardinal Glass	Jordan Lagerman
Centre For Research and Developement Foundation	Yashkumar Shukla
Centro Brasileiro de Eficiência Energética em Edificações-CB3E	Saulo Guths
China Building Materials Test and Certification Group Co., Ltd. (ctc)	Wu,Jie
China Southern Glass Holding Company,Ltd	Chengde Huang
Corning Research & Development Corporation	J. Gregory Couillard
Eastman Chemical Company	Julia Schimmelpenningh
Eastman Chemical Company Performance Films DIvision	Beth Lawless-Coale
Emirates Float Glass	Arpan Basu
Erickson International	Justin Shjarback
Fraunhofer Institute for Solar Energy Systems	Helen Rose Wilson
Glas Trösch AG	Oliver Portmann
Guardian Glass LLC	Jason Theios, Eric Stuewer
Hankuk Glass Industries Inc.	Youngmi, Kim
ift Rosenheim GmbH	Michael Freinberger
INTERPANE Entwicklungs- und Beratungsgesellschaft	Dr. Hansjoerg Weis
Lawrence Berkeley National Laboratory	Jacob C. Jonsson
Madico Inc.	Jesse Manship and Stefan Setz
NSG Group (Pilkington)	James Farmer
Oceania Glass	Nicholas Trotter
Optical Data Associates, LLC	Michael R Jacobson
OTM Solutions Pte Ltd, Singapore	Chen Fangzhi
PFG Building Glass	Rahab Bopape
Pilkington Glass Russia LLC	Dmitriy Bernt

continued on next page

Institute	Contact
PT Asahimas Flat Glass Tbk	Alfan Bagus Win Hartono
SageGlass Saint Gobain	Robert Newcomb
Saint-Gobain Research	Loi-Brian Clemenceau
Solar Gard Saint Gobain	Miguel Detres
Sonnergy France	Charles Anderson
SYP GLASS GROUP CO.,LTD	Sun Dahai
Viracon	Mark Meuser
Vitro Architectural Glass	Michael Buchanan
Vitro S.A.B de C.V	José Cid
Yenisehir Regional Laboratory	Senem TIVECI-Mehmet Ali AK

B Graphs for all UV/Vis/NIR measurements

The graphs on following pages all show integrated solar and visible optical properties for each sample. The individual markers (squares and circles) show reported values, dotted lines show plus and minus two times the calculated standard deviation for that property, and finally dashed lines show limits imposed by NFRC 302 (.01 for transmittance and .02 for reflectance).

B.1 Sample #1

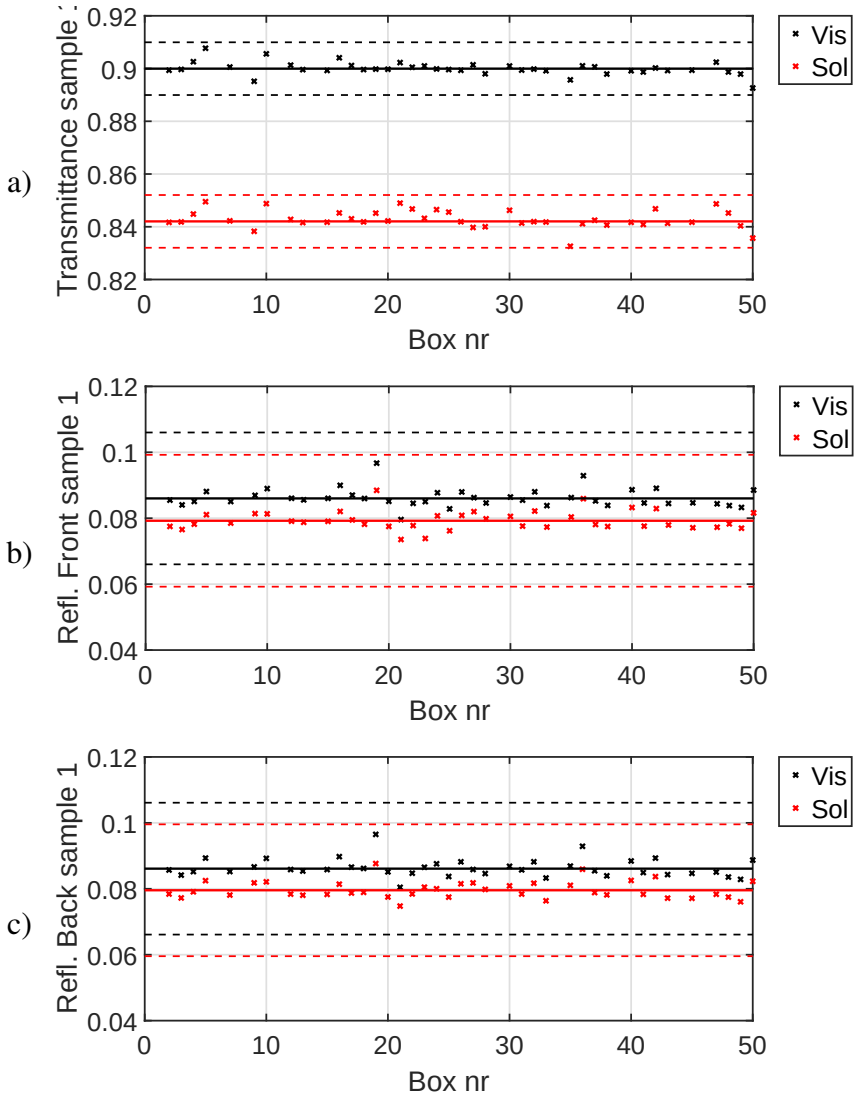

Figure 15: Integrated solar and visible optical properties for sample 1. a) Transmittance, b) front reflectance, and c) back reflectance.

B.2 Sample #2

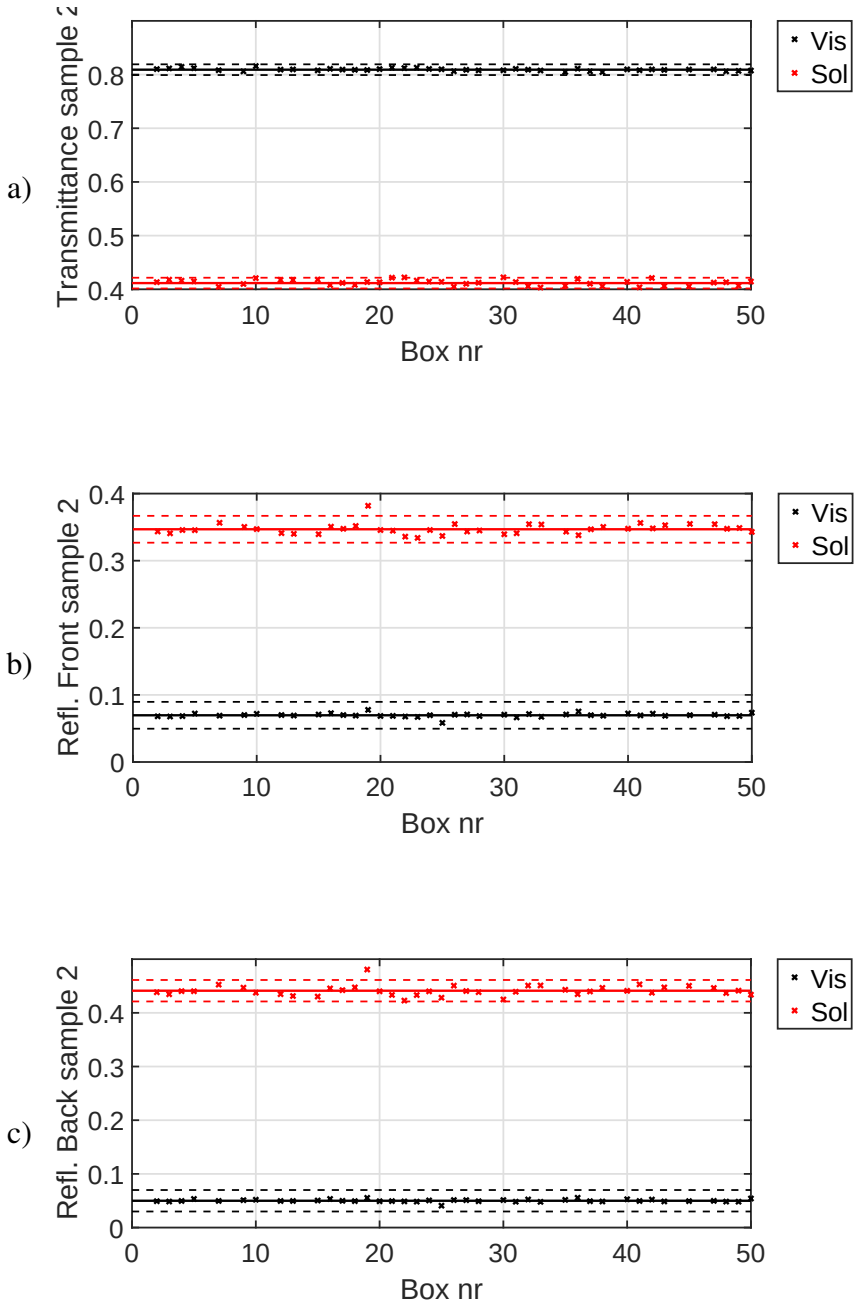

Figure 16: Integrated solar and visible optical properties for sample 2. a) Transmittance, b) front reflectance, and c) back reflectance.

B.3 Sample #3

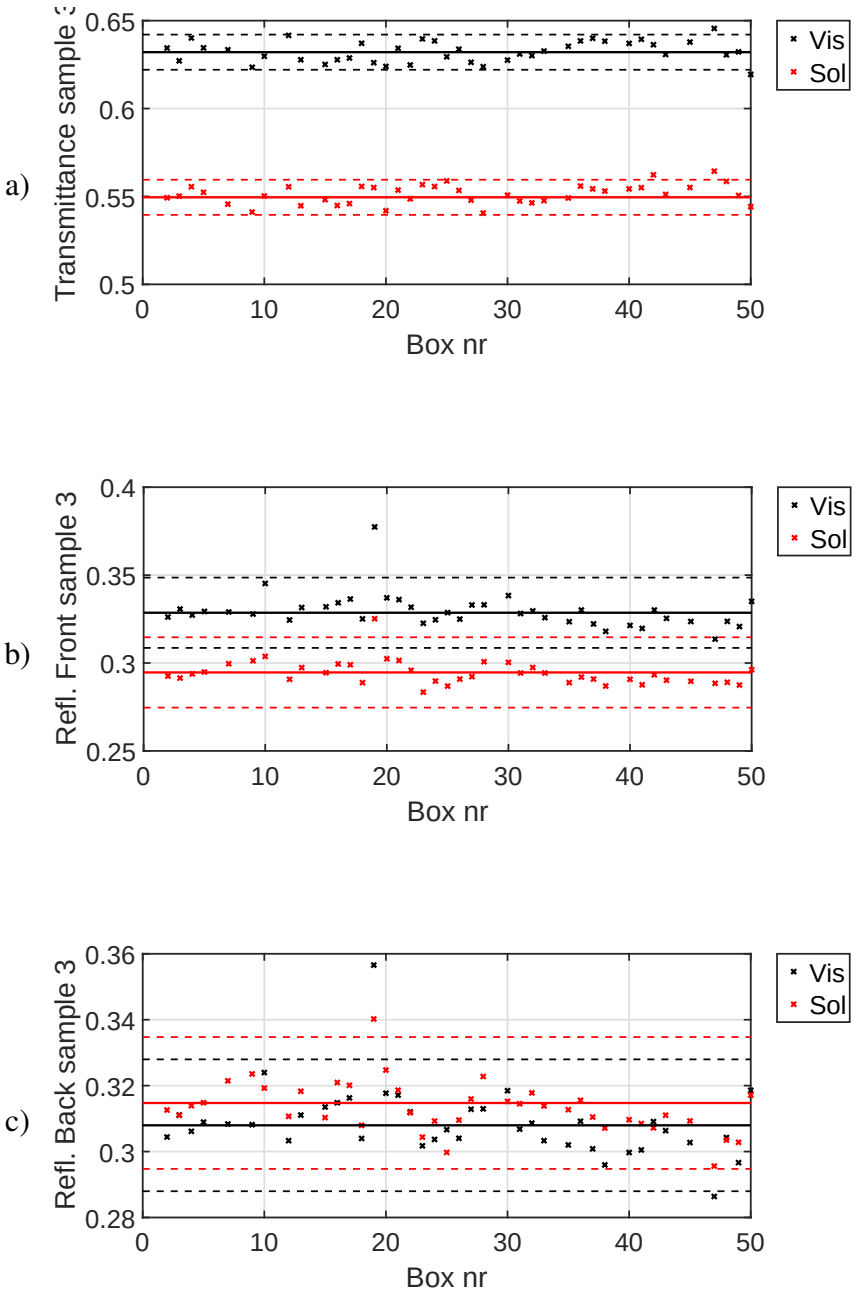

Figure 17: Integrated solar and visible optical properties for sample 3. a) Transmittance, b) front reflectance, and c) back reflectance.

C Graphs for all IR measurements

The graphs in this section shows the calculated emissivity according to NFRC 301. Only one of the five uncoated glass surfaces are shown. The individual markers show reported values, dotted lines show plus and minus two times the calculated standard deviation for that property, and finally dashed lines show limits imposed by NFRC 302 (.02 for emissivity).

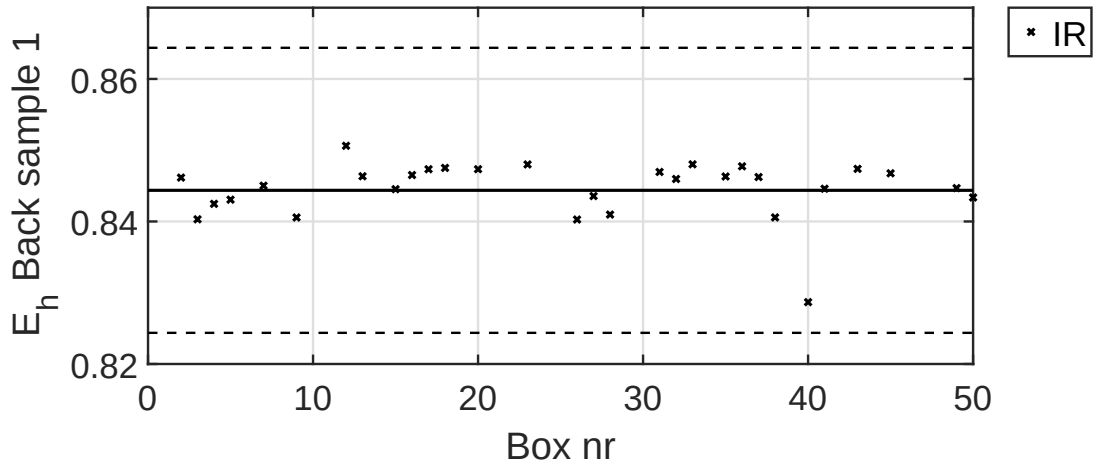

Figure 18: Calculated emissivity of sample 1.

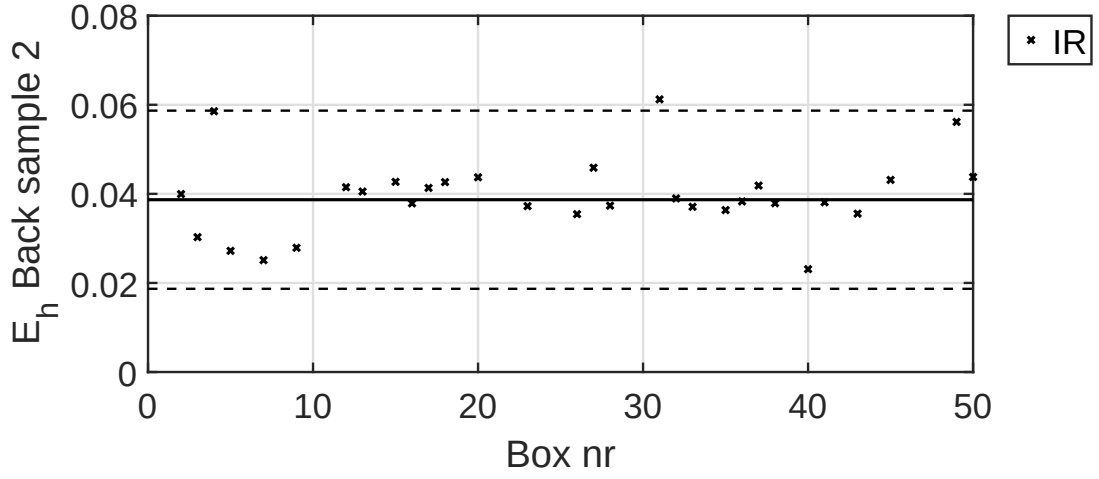

Figure 19: Calculated emissivity of of sample 2.

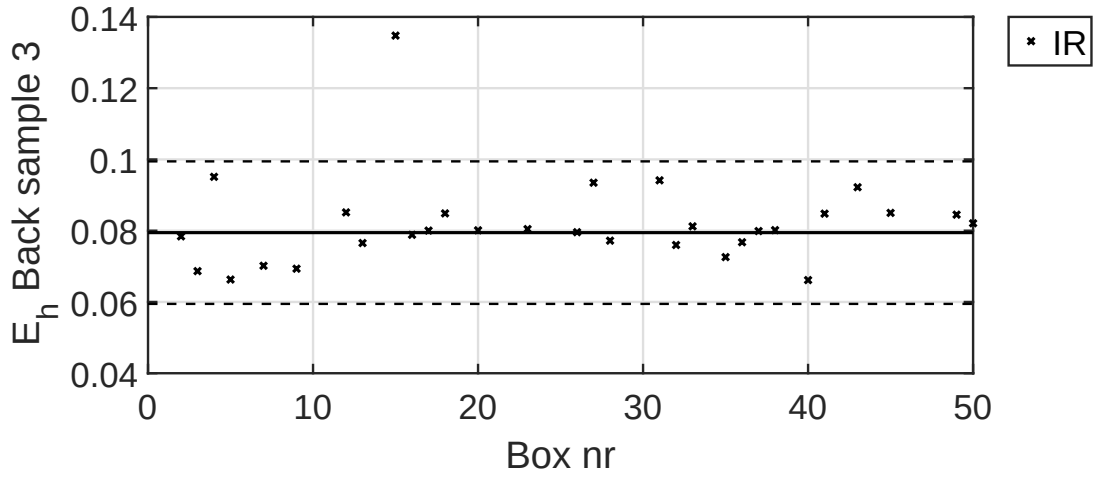

Figure 20: Calculated emissivity of sample 3.